14th International Symposium on Turbulence and Shear Flow Phenomena (TSFP14)
Heidelberg, Germany, July 28–31, 2026

VORTEX-ODOR DYNAMICS FROM BURST-AND-COAST MOTION OF AN ANGUILLIFORM SWIMMERS

Zahra Maleksabet
Nature-Inspired Engineering Research Lab (NIERL)
Department of Mechanical and Mechatronics Engineering
Lakehead University, Thunder Bay, Ontario P7B 5E1, Canada

Maham Kamran
Nature-Inspired Engineering Research Lab (NIERL)
Department of Mechanical and Mechatronics Engineering
Lakehead University, Thunder Bay, Ontario P7B 5E1, Canada

Ali Tarokh
Department of Mechanical and Mechatronics Engineering
Lakehead University, Thunder Bay, Ontario P7B 5E1, Canada

Muhammad Saif Ullah Khalid*
Nature-Inspired Engineering Research Lab (NIERL)
Department of Mechanical and Mechatronics Engineering
Lakehead University, Thunder Bay, Ontario P7B 5E1, Canada
*Email: mkhalid7@lakeheadu.ca

ABSTRACT

We investigate the coupling between vortex dynamics and transport of odor for burst-and-coast motion and continuous undulation of an anguilliform swimmer using high-fidelity three-dimensional simulations using an in-house sharp-interface immersed-boundary method-based solver coupled with the transport equation for odor dynamics, which enables simultaneous analysis of hydrodynamics and scalar transport. The simulations are performed at a Reynolds number of $\mathrm{Re} = 3000$ and a Strouhal number of $\mathrm{St} = 0.40$ for a range of values of duty cycle. Our results show that odor does not strictly follow vortex topology but resides predominantly within vortical structures, which confirms strong coupling between coherent flow features and transport of odor. At low duty cycle, intermittent vortex generation produces significant lateral spreading of odor. Nevertheless, the lack of temporal continuity limits its downstream persistence, resulting in weak transport. At intermediate duty-cycle values, increased interactions between successively shed vortices enhances both coherence and persistence of odor cues, leading to maximum effectiveness of its transport. On the contrary, continuous undulation produces a stable and streamwise-aligned wake that supports sustained transport of odor cues in the wake but confines its spatial distribution in the lateral direction. The present work provides new insight into the role of intermittent kinematics of a biological marine swimmer and the results unsteady vortex dynamics for transporting chemical cues in aquatic environments.

1 Introduction

Aquatic swimmers experience propulsion by producing traveling waves along their bodies, which interact with the surrounding fluid to form coherent vortical structures. These vortices govern the transfer of momentum between the swimmer and the fluid and determine wake topology, hydrodynamic forces, and propulsion efficiency. Previous studies investigated vortex dynamics in anguilliform and carangiform swimmers and showed that morphology and kinematics strongly influenced vortex formation, wake structure, and force production (Borazjani & Sotiropoulos, 2009; Khalid *et al.*, 2021*b*,*a*; Gazzola *et al.*, 2014). These studies demonstrated that anguilliform swimmers generated distributed vortical structures along their entire bodies, whereas carangiform swimmers produced concentrated vortices near the posterior region. The organization, strength, and convection of these vortices determine hydrodynamic performance and propulsion characteristics (Triantafyllou *et al.*, 2000; Sfakiotakis *et al.*, 1999; Lauder & Tytell, 2005; Fish & Lauder, 2017).

Many biological swimmers employ not only continuous undulation but also intermittent burst-and-coast motion. In this mode, swimmers alternate between an active burst phase and a passive coast phase (Wu, 2011; Dai *et al.*, 2018; Liu *et al.*, 2025; Li *et al.*, 2023; Yang *et al.*, 2024). A recent research work showed that burst-and-coast motion modified vortex topology and wake structure significantly compared to continuous motion (Maleksabet *et al.*, 2025). That study revealed that smaller values of duty cycle produced bow-shaped wakes with large lateral spreading, whereas increasing duty cycle aligned the vortex rows more closely with the streamwise direction. These changes in organization of vortices influenced hydrodynamic forces and wake stability. However, although vortex dynamics during burst-and-coast motion were examined in detail using both two- and three-dimensional simulation frameworks, the influence of this motion on transport of chemical cues in the wake remains unexplored (Dai *et al.*, 2018; Akoz & Moored, 2018; Li *et al.*, 2023; Yang *et al.*, 2024; Liu *et al.*, 2025; Maleksabet *et al.*, 2025).

Chemical sensing plays an important role in navigation, foraging, and communication for aquatic organisms (Cox, 2008; Brönmark & Hansson, 2012; Montgomery *et al.*, 2014; Cardé, 2021; Bleckmann *et al.*, 2001). A few recent studies investigated coupling between vortex dynamics and transport of odor for continuously undulating swimmers in both two- and three-dimensional configurations (Kamran *et al.*, 2024, 2025). These studies showed that odor plumes did not strictly follow vortex topology but broadly resided predominantly within the vortical structures, which indicated strong coupling between coherent flow features and transport of chemical cues. Furthermore, these studies demonstrated that a swimmer's kinematics significantly influenced spatial distribution and persistence of odor in the wake. However, these investigations focused on continuous undulation and did not consider transport of odor from a biological swimmer, when it performs burst-and-coast motion, which produces fundamentally different vortex dynamics from those of continuously undulating swimmers that may play a crucial role in underwater sensing (Bunnell *et al.*, 2011; Domenici *et al.*, 2011; Cardé, 2021; Anderson *et al.*, 2001; Videler, 1993; Lei *et al.*, 2023; Lei & Li, 2023).

The present work extends our previous investigations (Maleksabet *et al.*, 2025) by examining coupling between vortex dynamics and transport of odor during burst-and-coast motion and by comparing it with the phenomenon for a continuously undulating anguilliform swimmer. Burst-and-coast motion produces highly unsteady intermittent vortical structures, which influence transport, persistence, and spatial distribution of odor in the wake. Understanding this coupling provides insight into how kinematic strategies influence transport of chemical cues in aquatic environments. Due to its importance and relevance with respect to underwater biological sensing mechanisms, we make it the subject of our currently presented research.

The primary objectives of this work are to address the following questions: (i) how coupling between vortex dynamics and transport of odor evolves during burst-and-coast motion compared to continuous undulation, (ii) how duty cycle influences the strength, persistence, and spatial distribution of odor in the wake of an anguilliform swimmer, and (iii) which swimming strategy offers a more favorable balance between hydrodynamic performance and reduced odor detectability for design of autonomous underwater vehicles. To address these questions, we perform three-dimensional simulations using an in-house sharp-interface immersed-boundary method (IBM) based solver, VorteXdyn, for the fluid-body-odor interactions. This computational framework enables us to resolve vortex dynamics and transport of odor simultaneously and to identify the physical mechanisms that govern dispersion of chemical cues in biologically relevant swimming modes. Our findings are expected to contribute to the fields of marine biology, environmental conservation, and oceanographic exploration, while also aiding in the development of efficient and adaptive underwater robotic systems Bianchi *et al.* (2021); Marras & Porfiri (2012).

2 Computational Methodology

Here, we use the geometry of a real-like eel (*Anguilla rostrata*), as shown in Fig. 1, to represent the kinematic mode of anguilliform swimming. It was shown by Khalid *et al.* (2021*b*) that the discretized geometry of the eel could be represented using 33,112 triangular elements and 16,558 nodes. Generally, an eel undulates a large portion of its slender body to generate motion, where the amplitude profile of anguilliform kinematic is expressed by the following equation (Maertens *et al.*, 2017; Khalid *et al.*, 2020, 2021*b*):

$$A\left(\frac{x}{L}\right) = 0.0367 + 0.0323\left(\frac{x}{L}\right) + 0.0310\left(\frac{x}{L}\right)^2; \quad 0 < \frac{x}{L} < 1 \tag{1}$$

where, x represents the stream-wise coordinate of each node used to discretize the 3D model swimmer, and $A(x/L)$ denotes the local amplitude at a specific position along the swimmer's body, nondimensionalized by its total length (L).

For our study, we consider two different motions, continuous and burst-and-coast undulation, as explained by Kamran *et al.* (2024, 2025) and Maleksabet *et al.* (2025), respectively. For continuous undulation, we model the undulatory motion using f as the oscillation frequency, λ as the wavelength, t as the time, and $A(x/L)$ as the amplitude profile (Eq. 1):

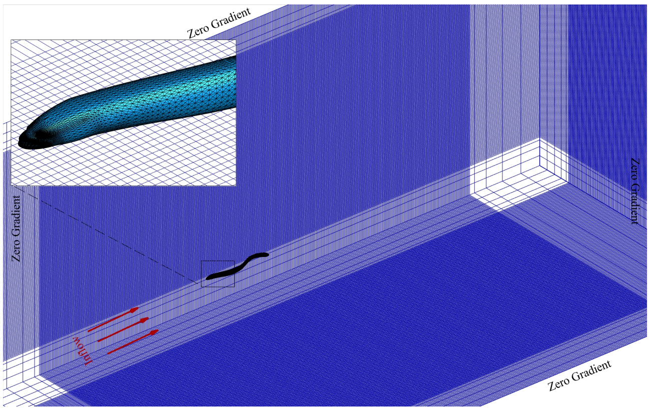

Figure 1: Computational domain and mesh with boundary conditions, including a zoomed-in view of an eel geometry with a triangular mesh.

$$y\left(\frac{x}{L}\right) = A\left(\frac{x}{L}\right)\sin\left[2\pi\left(\frac{x}{\lambda} - ft\right)\right] \tag{2}$$

For burst-and-coast undulation, each swimmer's body kinematics follows a wavy motion defined by a traveling wave function combined with a temporal smoothing function to transition between the burst and coast phases. This formulation is primarily based on the approach proposed by Yang *et al.* (2024) and also followed by Maleksabet *et al.* (2025). Equation 3 describes the instantaneous local undulatory kinematics at each point on a swimmer's body:

$$y(x,t) = \begin{cases} S(t)A(x)\sin\left[2\pi\left(\frac{x}{\lambda} - \frac{t}{T_s}\right) - \frac{2\pi}{\lambda}\right]; & 0 \le t \le T_s \\ 0; & T_s < t \le T \end{cases} \tag{3}$$

A cosine-based smoothing function modulates the undulatory kinematics during the burst phase:

$$S(t) = \begin{cases} 0.5\left[1 - \cos\left(\frac{4\pi t}{T_s}\right)\right]; & 0 \le t \le 0.25T_s \\ 1, & 0.25T_s < t \le 0.75T_s \\ 0.5\left[1 - \cos\left(\frac{4\pi t}{T_s}\right)\right]; & 0.75T_s < t \le T_s \end{cases} \tag{4}$$

In the equations above, T_s shows the time for the burst phase in one full burst-and-coast cycle, for which T is the total period. To make the comparison of the intermittent swimming with that of continuous undulations, the undulation frequency, f, is defined as the reciprocal of the total time period encompassing both the burst and coast phases ($f = 1/T$). Therefore, the non-dimensional quantity, duty cycle (DC), represents the fraction of the time spent for active undulation within a swimming cycle, as shown in Fig. 2. It is defined below (Akoz & Moored, 2018):

$$DC = \frac{\text{Time for active undulation during burst}}{\text{total time for one burst-and-coast cycle}} = \frac{T_s}{T} \tag{5}$$

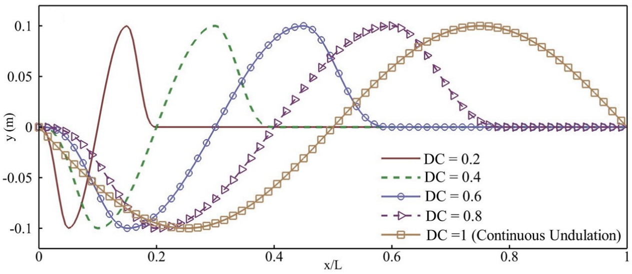

Figure 2: The kinematic profiles of the swimmer's tail during burst-and-coast motion with different duty cycles

The governing mathematical model for fluid flows is based on the following non-dimensional forms of the continuity and incompressible Navier-Stokes equations (Mittal *et al.*, 2008; Farooq *et al.*, 2025):

$$\frac{\partial u_j}{\partial x_j} = 0, \quad (6)$$

$$\frac{\partial u_i}{\partial t} + u_j \frac{\partial u_i}{\partial x_j} = -\frac{1}{\rho}\frac{\partial p}{\partial x_i} + \frac{1}{Re}\frac{\partial^2 u_i}{\partial x_j \partial x_j} + f_b, \quad (7)$$

where $\{i,j\} = \{1,2,3\}$, x_i represents the Cartesian directions, u_i denotes the Cartesian components of velocity of the fluid, p is the pressure, and Re is the Reynolds number. We define it as $\mathrm{Re} = U_\infty L/\nu$, where U_∞ shows the free-stream velocity, and ν is kinematic viscosity of the fluid. In this formulation, f_b is a discrete forcing term that enables a sharp representation of the immersed boundary (Mittal *et al.*, 2008; Farooq *et al.*, 2025). We solve these governing equations using a sharp-interface IBM on a non-uniform Cartesian grid. Radial basis functions serve as the interpolation scheme to precisely identify the immersed bodies (Farooq *et al.*, 2025). A central difference scheme is employed for spatial discretization of the diffusion term, while the Quadratic Upstream Interpolation for Convective Kinematics (QUICK) scheme is used for the convection term. Temporal integration is performed using a fractional-step method, achieving second-order accuracy in both time and space. The wavy kinematics are prescribed as a boundary condition on the swimmer's body through a ghost-cell technique (Farooq *et al.*, 2025), which accommodates both rigid and flexible structures. Neumann boundary conditions are applied at the far-field boundaries, except at the left-side inlet boundary, where Dirichlet conditions specify the inflow. Further details of this fully parallelized solver and its application to various bio-inspired fluid-structure interactions related problems are provided by Farooq *et al.* (2025).

Chemical sensing plays a crucial role in navigation, foraging, and communication by diffusion and advection of chemical cues released in the fluid surrounding a swimmer. In this work, we model the dynamics of odor using the chemical transport equation to determine the instantaneous odor concentration field in the entire computational domain. The governing equation for the unsteady convection-diffusion of the odorant is as follows:

$$\frac{\partial C}{\partial t} + u_i \frac{\partial C}{\partial x_i} = D \frac{\partial^2 C}{\partial x_i \partial x_i}, \quad (8)$$

where, C represents the odor concentration, nondimensionalized by the uniform source concentration at the swimmer's body surface ($C_\Omega = 1$), and D denotes the diffusion coefficient of the odor. The odor field is modeled with a Dirichlet boundary condition, where a constant concentration is applied on the fish surface to represent a continuous source of chemical cues. The temporal term (first term on the left-hand side), the convective term (second term on the left-hand side), and the diffusion term (on the right-hand side) in Eq. 8 are discretized using the same computational schemes applied to the Navier-Stokes equations (Eq. 7). This robust computational framework enables multi-physics simulations involving fluid-structure-chemical interactions, allowing the accurate modeling of odor transport in vortex-dominated flows. The interplay of convection and diffusion processes is analyzed to describe transport of odor within the flow field, explaining important physical mechanisms that drive underwater chemical sensing for biological marine species. To ensure the accuracy and reliability of the numerical results, extensive grid-independence and time-step convergence studies are performed. For verification and validation of our computational methodology, we refer the reader to the studies of Farooq *et al.* (2025), Kamran *et al.* (2024), and Maleksabet *et al.* (2025).

3 Results and Discussion

To address the research questions, the simulations are performed at Re = 3000 and a Strouhal number (St) of 0.40. We define the Strouhal number as $\mathrm{St} = 2A_\circ f/U_\infty$, where $A_\circ$ is the one-sided peak amplitude at the swimmer's trailing edge. Figure 3 shows the topology of vortices using the Q-criterion along with isosurfaces of non-dimensional odor concentration. At a low value of duty cycle (DC = 0.2, Fig. 3(a)), vortex activity is strong and highly unsteady due to intermittent forcing. The wake exhibits a bow-shaped structure with significant lateral separation of vortices, consistent with previous observations by Maleksabet *et al.* (2025). This lateral separation promotes spanwise spreading of odor, but the distribution of odor remains weak and fragmented. The interruption of undulation during the coast phase limits sustained transport of odor, which reduces persistence in the downstream direction despite the presence of energetic vortices.

As duty cycle increases (DC = 0.4–0.8, Fig. 3(b)–(d)), vortex structures become more connected and progressively align in the streamwise direction. The bow-shaped organization weakens, and the spacing between vortices decreases, which enhances interaction between successive vortices. This increased interaction improves transport of odor and results in larger and more coherent regions of high concentration in the wake. At the same time, spanwise spreading of odor decreases as the wake becomes more organized and less laterally dispersed. For continuous undulation (DC = 1.0, Fig. 3(e)), vortex shedding becomes continuous and forms a stable and nearly aligned wake to the streamwise direction. The odor field forms a confined and elongated structure downstream of the swimmer. In this case, spanwise spreading is minimal compared to burst-and-coast motion. This transition in wake topology indicates that duty cycle not only alters the strength of the vortices but also changes how vortices are arranged and how long they remain dynamically relevant in the wake. At low

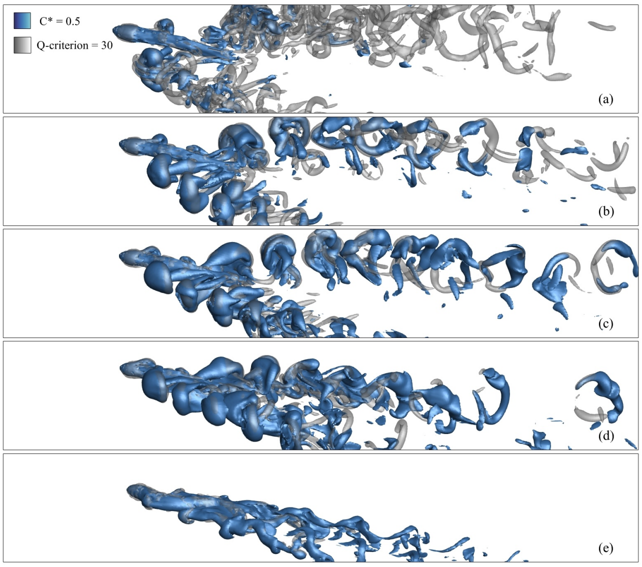

Figure 3: Topology of vortices visualized using the Q-criterion with a threshold value of 30. Panels (*a*–*e*) correspond to duty-cycle values of $\mathrm{DC} = 0.2, 0.4, 0.6, 0.8,$ and 1.0 for an eel.

duty cycle, the interruption of body undulation produces isolated vortical structures that convect away without maintaining a persistent pathway for transport of odor. As the duty cycle increases, the reduced temporal gap between successive burst events allows the newly generated vortices to interact more directly with the previously formed wake. This process promotes a more continuous transport pathway in the streamwise direction and enables odor to remain embedded within coherent flow structures over a longer downstream distance. Therefore, the observed increase in coherence of odor at intermediate and high duty-cycle values is associated not only with stronger advection but also with improved continuity of the wake.

To understand the hydrodynamic performance, we calculate the cycle-averaged drag coefficient over the last five cycles for the anguilliform swimmer. Figure 4 shows that as duty cycle increases, the cycle-averaged drag decreases, indicating improved propulsive performance for higher duty-cycle and continuous undulation. At $\mathrm{DC} = 1.0$, the cycle-averaged drag approaches a near-balanced condition, which suggests a condition for self propulsion where thrust and drag are nearly balanced over a cycle. Contrarily, the cases with lower duty cycles are characterized by intermittent forcing, where the burst phase generates strong acceleration of the surrounding fluid, followed by deceleration during the coast phase. This intermittency produces more impulsive force variations, which results in a higher cycle-averaged drag. As duty cycle increases from $\mathrm{DC} = 0.2$ to 0.8, the magnitude of these impulsive effects reduces, and the force response transitions toward a more continuous and stable behavior. This trend reflects a shift from highly transient vortex generation at a low duty cycle to more coherent and sustained vortex shedding at the greater values of duty cycle. Consequently, although lower duty-cycle cases generate strong instantaneous vortex activity, they do not produce superior hydrodynamic performance due to the lack of temporal and spatial continuity of the wake. This behavior highlights that hydrodynamic performance improves with increasing duty cycle. From a hydrodynamic perspective, higher duty-cycle cases are favorable because they reduce fluctuations in forces and help the swimmer move toward a better thrust-generating propulsive state.

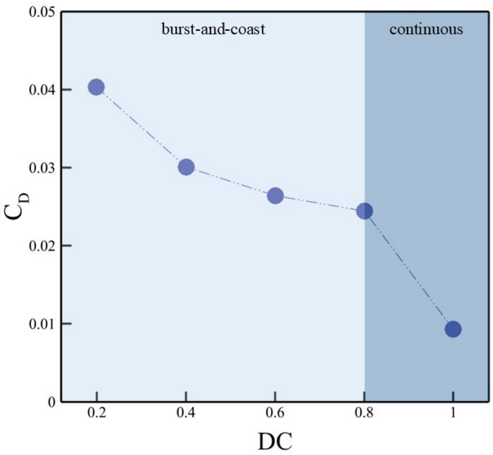

Figure 4: Time-averaged drag coefficient of the eel.

To examine the coupling between vortex dynamics and transport of odor, we analyze the spatial distribution of odor in the wake. In particular, we consider a cross-sectional plane at a distance of $x/L = 2.5$ from the swimmer's trailing edge, as shown in Fig. 5, to quantify the spanwise distribution and lateral spreading of odor. This plane allows us to isolate the influence of vortex structures on the spanwise distribution of odor. Figure 5 shows that at a low value of duty cycle ($\mathrm{DC} = 0.2$), odor spreads over a wider spanwise region despite its lower overall concentration. This behavior is consistent with the bow-shaped vortex structures observed in Fig. 3, where lateral separation of vortices promotes cross-stream transport of odor. As duty cycle increases ($\mathrm{DC} = 0.4$–0.8), the spanwise extent of odor decreases, while the concentration becomes more localized and coherent. The reduction in lateral vortex separation leads to a more confined distribution of odor, indicating a transition from a laterally dispersed wake to a more organized flow structure. For continuous undulation ($\mathrm{DC} = 1.0$), odor is concentrated within a narrow region with minimal spanwise spread. The distribution appears more compact and aligned with the centerline, which reflects the absence of intermittent vortex structures that promote lateral dispersion.

To quantify the observed behavior, we use the effectiveness of odor, C^*_{eff} proposed by Kamran *et al.* (2025), as shown in Fig. 6. The normalized effectiveness of odor is defined as $C^*_{\mathrm{eff}} = \frac{A_{\mathrm{iso}}}{A_{\mathrm{fish}}}$, where A_{iso} represents the isosurface area of odor within a given subzone, and A_{fish} denotes the body area of the swimmer. We divide the wake region, starting from the trailing edge of the swimmer, into 10 subregions, each with a length of $0.5L$, which covers the wake up to $5.5L$ downstream. For this analysis, we extract the isosurface corresponding to $C^* = 0.5$ and evaluate its spatial distribution within each subregion. Figure 6 exhibits that C^*_{eff} for $\mathrm{DC} = 0.2$ remains significantly lower than all other cases, including continuous undulation. This result confirms that strong but intermittent vortex activity at low duty cycle does not sustain transport of odor in the downstream direction. As duty cycle increases ($\mathrm{DC} = 0.4$–0.8), C^*_{eff} increases substantially, particularly in the near wake. These cases exhibit higher effectiveness of odor compared to continuous motion, which highlights that a balance between vortex interaction and intermittency enhances

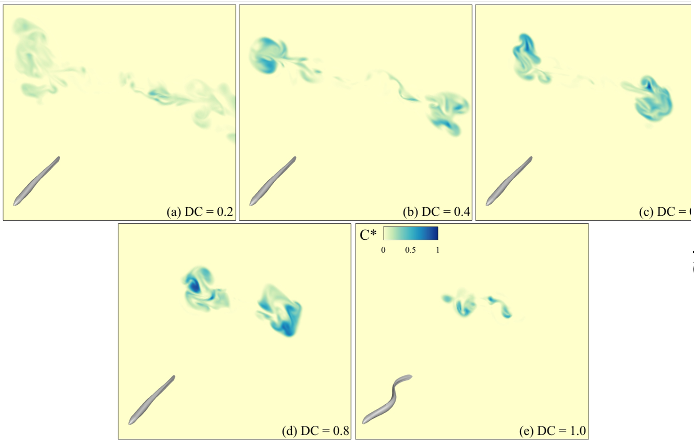

Figure 5: Odor plumes on a plane located at a distance of $x/L = 2.5$ from the swimmer at different values of DC for St = 0.4.

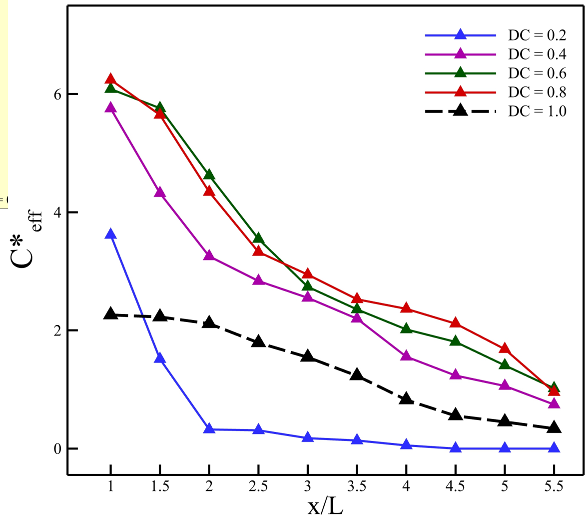

Figure 6: Effectiveness of odor for different duty-cycle values for an eel.

transport of odor. Our results suggest that an intermediate duty cycle produces conditions that maximize persistence and spatial coverage of odor. For continuous undulation (DC = 1.0), C^*_{eff} decreases gradually along the streamwise direction and remains lower than the intermediate duty-cycle cases. Although continuous motion produces a stable wake, the reduced spanwise spreading limits the overall effectiveness of odor distribution. These quantitative results are consistent with the observations from Fig. 3 and Fig. 5, which showed that lower duty cycle produces wider but weaker distribution, while intermediate duty cycle enhances both coherence and persistence of odor in the wake. On one hand, intermittent motion enhances lateral redistribution of odor by producing separated vortical structures and unsteady cross-stream motion. On the other hand, excessive intermittency shortens the active transport phase and weakens the continuity of odor advection in the downstream direction. As a result, very low duty-cycle motion spreads odor over a wider region but does not sustain sufficiently strong concentrations far downstream. Continuous undulation, in contrast, maintains downstream transport but confines the odor field to a relatively narrow region. Intermediate duty-cycle values seems to provide the most favorable balance between these two mechanisms by preserving both wake coherence and sufficient lateral spreading, which explains the larger values of C^*_{eff} observed in these cases.

The combined observations from Figs. 3, 5, and 6 directly address the primary research questions by clarifying how vortex dynamics govern the transport of odor under different kinematic conditions. The results show that coupling between vortex dynamics and transport of odor remains strong across all cases, as odor consistently resides within vortical structures. However, the effectiveness of this coupling depends on the temporal continuity and interaction of these structures. At low duty cycle (DC = 0.2), strong but highly intermittent vortex generation produces significant lateral spreading of odor. However, the interruption of undulation limits the persistence of these structures, which results in weak downstream transport and low effectiveness of odor. As duty cycle increases (DC = 0.4–0.8), enhanced interaction between successive vortices promotes both coherence and continuity in the wake. This balance leads to the highest intensity and persistence of odor, as reflected in the increased values of C^*_{eff}. These cases demonstrate that effective transport of odor requires not only strong vortices but also sustained interactions between them. For continuous undulation (DC = 1.0), the wake becomes stable and streamwise-aligned, which supports continuous downstream transport of odor. However, the absence of intermittency reduces lateral dispersion, resulting in a confined distribution of odor with lower overall spatial coverage compared to intermediate duty-cycle cases. These findings indicate that duty cycle governs the balance between vortex strength, vortex interaction, and intermittency, which collectively determine the intensity, persistence, and spatial distribution of odor in the wake. While lower duty-cycle motion enhances lateral spreading without sufficient persistence, and continuous motion ensures persistence with limited spreading, intermediate duty-cycle provides the most effective combination of both mechanisms.

4 Conclusion

We investigate the coupling between vortex dynamics and transport of odor for burst-and-coast motion and continuous undulation in an anguilliform swimmer. The results show that vortex structures govern transport pathways of odor, while duty cycle controls their effectiveness by altering vortex interaction and temporal continuity. Low duty-cycle motion produces strong but intermittent vortices that enhance lateral spreading but limit downstream persistence of odor. Continuous undulation produces a stable and streamwise-aligned wake that supports sustained transport but restricts spanwise distribution. Intermediate duty-cycle values provide the most effective balance between these mechanisms by maintaining both coherence and interaction of vortices, which results in the highest intensity and persistence of odor in the wake. These findings demonstrate that transport of odor in unsteady swimming is governed by the interplay between strength of vortices in terms of size and vorticity magnitude, interference mechanism between them, and intermittency of the undulatory kinematics. With respect to the balance between hydrodynamic performance and reduced odor detectability, continuous undulation provides the lowest drag and therefore the most efficient propulsion, while producing a relatively confined distribution of odor. However, it does not minimize odor intensity in absolute terms, as very low duty-cycle motion yields lower overall odor levels at the expense of persistence and propulsion efficiency. By controlling kinematic parameters, such as duty cycle, biological marine swimmer may regulate the transport and detectability of chemical cues while maintaining greater thrust for effective propulsion. This capability can enhance performance and operational safety in applications, such as underwater exploration, environmental monitoring, and coordinated navigation in complex aquatic environments.

REFERENCES

Akoz, Emre & Moored, Keith W 2018 Unsteady propulsion by an intermittent swimming gait. *Journal of Fluid Mechanics* **834**, 149–172.

Anderson, Erik J, Mcgillis, Wade R & Grosenbaugh, Mark A 2001 The boundary layer of swimming fish. *Journal of Experimental Biology* **204** (1), 81–102.

Bianchi, Giovanni, Cinquemani, Simone & Resta, Ferruccio 2021 Bio-inspired design of an underwater robot exploiting fin undulation propulsion. *Applied Sciences* **11** (6), 2556.

Bleckmann, Horst, Mogdans, Joachim & Dehnhardt, Guido 2001 Lateral line research: the importance of using natural stimuli in studies of sensory systems. In *Ecology of sensing*, pp. 149–167. Springer.

Borazjani, Iman & Sotiropoulos, Fotis 2009 Numerical investigation of the hydrodynamics of anguilliform swimming in the transitional and inertial flow regimes. *Journal of Experimental Biology* **212** (4), 576–592.

Brönmark, Christer & Hansson, Lars-Anders 2012 Aquatic chemical ecology: new directions and challenges for the future. *Chemical ecology in aquatic systems* pp. 272–278.

Bunnell, Toni, Hanisch, Kerstin, Hardege, Jörg D & Breithaupt, Thomas 2011 The fecal odor of sick hedgehogs (erinaceus europaeus) mediates olfactory attraction of the tick ixodes hexagonus. *Journal of chemical ecology* **37**, 340–347.

Cardé, Ring T 2021 Navigation along windborne plumes of pheromone and resource-linked odors. *Annual Review of Entomology* **66** (1), 317–336.

Cox, Jonathan PL 2008 Hydrodynamic aspects of fish olfaction. *Journal of the Royal Society Interface* **5** (23), 575–593.

Dai, Longzhen, He, Guowei, Zhang, Xiang & Zhang, Xing 2018 Intermittent locomotion of a fish-like swimmer driven by passive elastic mechanism. *Bioinspiration & biomimetics* **13** (5), 056011.

Domenici, Paolo, Blagburn, Jonathan M & Bacon, Jonathan P 2011 Animal escapology i: theoretical issues and emerging trends in escape trajectories. *Journal of Experimental Biology* **214** (15), 2463–2473.

Farooq, Hamayun, Akhtar, Imran, Hemmati, Arman & Khalid, Muhammad Saif Ullah 2025 An accurate immersed boundary method using radial-basis functions for incompressible flows. *Journal of Computational Physics* **531**, 113928.

Fish, Frank E & Lauder, George V 2017 Control surfaces of aquatic vertebrates: active and passive design and function. *Journal of Experimental Biology* **220** (23), 4351–4363.

Gazzola, Mattia, Argentina, Médéric & Mahadevan, Lakshminarayanan 2014 Scaling macroscopic aquatic locomotion. *Nature Physics* **10** (10), 758–761.

Kamran, Maham, Fardi, Amirhossein, Li, Chengyu & Khalid, Muhammad Saif Ullah 2024 How does vortex dynamics help undulating bodies spread odor? *Physics of Fluids* **36** (11).

Kamran, Maham, Fardi, Amirhossein, Li, Chengyu & Khalid, Muhammad Saif Ullah 2025 On the role of morphology and kinematics of biological swimmers to spread and suppress their odors in the wake. *arXiv preprint arXiv:2503.14648* .

Khalid, Muhammad Saif Ullah, Wang, Junshi, Akhtar, Imran, Dong, Haibo, Liu, Moubin & Hemmati, Arman 2021*a* Larger wavelengths suit hydrodynamics of carangiform swimmers. *Physical Review Fluids* **6** (7), 073101.

Khalid, Muhammad Saif Ullah, Wang, Junshi, Akhtar, Imran, Dong, Haibo, Liu, Moubin & Hemmati, Arman 2021*b* Why do anguilliform swimmers perform undulation with wavelengths shorter than their bodylengths? *Physics of Fluids* **33** (3).

Khalid, Muhammad Saif Ullah, Wang, Junshi, Dong, Haibo & Liu, Moubin 2020 Flow transitions and mapping for undulating swimmers. *Physical Review Fluids* **5** (6), 063104.

Lauder, George V & Tytell, Eric D 2005 Hydrodynamics of undulatory propulsion. *Fish physiology* **23**, 425–468.

Lei, Menglong & Li, Chengyu 2023 Wings and whiffs: Understanding the role of aerodynamics in odor-guided flapping flight. *Physics of Fluids* **35** (12).

Lei, Menglong, Willis, Mark A, Schmidt, Bryan E & Li, Chengyu 2023 Numerical investigation of odor-guided navigation in flying insects: Impact of turbulence, wingbeat-induced flow, and schmidt number on odor plume structures. *Biomimetics* **8** (8), 593.

Li, Gen, Kolomenskiy, Dmitry, Liu, Hao, Godoy-Diana, Ramiro & Thiria, Benjamin 2023 Intermittent versus continuous swimming: An optimization tale. *Physical Review Fluids* **8** (1), 013101.

Liu, Ruosi, Yang, Qiye, Ding, Yang & Xie, Guangming 2025 Intermittent swimming demonstrates energy-saving capabilities: experimental evidence from robotic fish. *Ocean Engineering* **340**, 122335.

Maertens, Audrey P, Gao, Amy & Triantafyllou, Michael S 2017 Optimal undulatory swimming for a single fish-like body and for a pair of interacting swimmers. *Journal of Fluid Mechanics* **813**, 301–345.

Maleksabet, Zahra, Kamran, Maham, Tarokh, Ali & Khalid, Muhammad Saif Ullah 2025 Vortex dynamics from burst-and-coast motion of anguilliform and carangiform swimmers. *arXiv preprint arXiv:2512.03969* .

Marras, Stefano & Porfiri, Maurizio 2012 Fish and robots swimming together: attraction towards the robot demands biomimetic locomotion. *Journal of The Royal Society Interface* **9** (73), 1856–1868.

Mittal, Rajat, Dong, Haibo, Bozkurttas, Meliha, Najjar, FM, Vargas, Abel & Von Loebbecke, Alfred 2008 A versatile sharp interface immersed boundary method for incompressible flows with complex boundaries. *Journal of computational physics* **227** (10), 4825–4852.

Montgomery, John, Bleckmann, Horst & Coombs, Sheryl 2014 Sensory ecology and neuroethology of the lateral line. *The lateral line system* pp. 121–150.

Sfakiotakis, Michael, Lane, David M & Davies, J Bruce C 1999 Review of fish swimming modes for aquatic locomotion. *IEEE Journal of oceanic engineering* **24** (2), 237–252.

Triantafyllou, Michael S, Triantafyllou, GS & Yue, Dick KP 2000 Hydrodynamics of fishlike swimming. *Annual review of fluid mechanics* **32** (1), 33–53.

Videler, John J 1993 *Fish swimming*, , vol. 10. Springer Science & Business Media.

Wu, Theodore Yaotsu 2011 Fish swimming and bird/insect flight. *Annual review of fluid mechanics* **43** (1), 25–58.

Yang, Dewu, Wu, Jie, Khedkar, Kaustubh, Chao, Li-Ming & Bhalla, Amneet Pal Singh 2024 Hydrodynamics and scaling laws for intermittent s-start swimming. *Journal of Fluid Mechanics* **984**, A2.